RESEARCH PAPER

Acta Neurobiol Exp 2022, 82: 65–76
DOI: 10.55782/ane-2022-006

Apelin-13 ameliorates LPS-induced BV-2 microglia inflammatory response through promoting autophagy and inhibiting H3K9ac enrichment of TNF-α and IL-6 promoter

Qing-Ming Peng[1], Jia-Hui Zhou[1], Zhe-Wei Xu[2], Qian-Cheng Zhao[3], Zhi-Yue Li[1]*, Qun Zhao[4]*

[1] Department of Spine Surgery, Third Xiangya Hospital of Central South University, Changsha, China,
[2] Department of Orthopedics and Traumatology, Hunan Chest Hospital, Changsha, China,
[3] Department of Orthopedics, The Second Affiliated Hospital of Sun Yat-Sen University, Guangzhou, China,
[4] Health Management Center, Third Xiangya Hospital of Central South University, Changsha, China,
** Email: lizhiyuecs@163.com; zhaoqunhy@163.com*

Microglia is activated and polarized to pro-inflammatory M1 phenotype or anti-inflammatory M2 phenotype in neuroinflammation. Apelin-13 exerts protective properties against neuroinflammation in several neurological disorders. We aimed to investigate whether apelin-13 played a protective role on BV-2 microglia and explore its underlying mechanisms. Lipopolysaccharide (LPS)-stimulated BV-2 microglia cells were treated with apelin-13. Microglia activation was evaluated by immunofluorescence with F-actin. Western blot was performed to measure the expression of autophagy associated proteins. CD16/32 and CD206 were detected to assess microglia polarization by western blot and flow cytometry. qRT-PCR was utilized to measure inducible nitric oxide synthase (iNOS), arginase-1 (Arg-1), interleukin-10 (IL-10), interleukin-6 (IL-6) and tumor necrosis factor-alpha (TNF-α). Histone H3 acetyl lysine 9 (H3K9ac) enrichment of TNF-α and IL-6 promoter was detected by ChIP. We discovered that apelin-13 impacted the actin cytoskeleton, recovering the control phenotype following LPS exposure. Apelin-13 improved autophagy-mediated microglia polarization towards M2 phenotype to alleviate inflammatory response in LPS-stimulated cells. Autophagy flux inhibitor chloroquine antagonized these effects of apelin-13 on LPS-stimulated cells. Besides, apelin-13 decreased the enrichment of H3K9ac at the promoter region of TNF-α and IL-6 to inhibit inflammatory response, which was reversed by histone deacetylase antagonist valproate. Taken together, apelin-13 alleviated inflammation *via* facilitating microglia M2 polarization due to autophagy promotion, and inhibiting H3K9ac enrichment on promoter regions of TNF-α and IL-6.

Key words: apelin-13, microglia polarization, autophagy, H3K9ac, inflammation

INTRODUCTION

Microglia, acting as immune-competent cells, are involved in maintaining normal function in brain (Wolf et al., 2017). Microglia activation is heterogeneous with different functional phenotypes of M1 phenotype, acting as a pro-inflammatory role, and M2 phenotype, acting as an immunosuppressive role (Yu et al., 2019: Tang and Le, 2016). Microglia activation of M1-phenotype leads to neuronal dysfunction, injury and degeneration. M1-polarized microglia aggravates neuronal death induced by oxygen glucose deprivation (Hu et al., 2012). However, M2 microglia-derived exosomes alleviate ischemic brain injury and increase neuronal survival (Song et al., 2019). The inhibition of microglia polarization to M1 phenotype prevents oligodendrocytes necroptosis in spinal cord injury (SCI) rats (Fan et al., 2019). Furthermore, microglia polar-

Received 18 January 2021, accepted 10 August 2021

ization from M1 to M2 state alleviates SCI (Han et al., 2018). Recovery of motor function is promoted after M2-deviated microglia transplantation in SCI mice (Kobashi et al., 2020). Modulating the polarization of microglia may be a promising avenue for treating neurological disorders including SCI.

Autophagy is a catabolic process playing essential roles in keeping cellular homeostasis in physiological and pathological conditions (Livingston and Dong, 2014). Autophagy is implicated in regulation of microglia polarization in neuroinflammation attenuation (Zhuang et al., 2020). Salidroside activates autophagic flux, participating in microglia polarization to attenuate neuroinflammation after SCI (Wang et al., 2018). Toll-like receptor 2 (TLR2)-mediated autophagic signaling regulates inflammatory response to activate microglial M1/M2 switching (Ma et al., 2020). Lipopolysaccharide (LPS), a major cell wall component in gram-negative bacteria, is a potent stimulator for microglial activation, which leads to inflammatory response that accelerates the progression of neurological disorders (Nam et al., 2018; Do et al., 2020). LPS leads to microglia M1 polarization as well as autophagy inhibition (Ji et al., 2018). Enhanced microglia autophagy decreases neuroinflammation induced by LPS (Ye et al., 2020). Microglia stimulated by LPS transforms to M1 phenotype to generate M1 related factors, including proinflammatory cytokines tumor necrosis factor-alpha (TNF-α), interleukin-6 (IL-6) and interleukin-1beta (IL-1β) (Orihuela et al., 2016), contributing to neuronal damage (An et al., 2020). In adult rats with neonatal alcohol pre-exposure, hypothalamic microglia show the increased histone H3 acetyl lysine 9 (H3K9ac) enrichment at promoter regions of TNF-α and IL-6 and the up-regulated expression of TNF-α and IL-6 after LPS treatment (Chastain et al., 2019). These researches illustrate that LPS promotes microglia inflammatory response possibly *via* two ways: promoting microglia M1 polarization by inhibiting autophagy; increasing H3K9ac enrichment at TNF-α and IL-6 promoter regions.

Apelin, acting as an endogenous ligand of apelin receptor, is widely distributed in neuronal cell bodies and fibers (Zhang et al., 2015). Apelin-13 suppresses microglia activation to attenuate brain edema and preserve blood-brain barrier integrity, exerting the neuroprotective effects (Xu et al., 2019). Apelin-13 alleviates neuroinflammation through decreasing M1 marker CD86 and increasing M2 marker CD206 of N9 microglia (Zhou et al., 2019). Additionally, apelin-13 protects dopaminergic neurons *via* reversing the reduced autophagy induced by 1-methyl-4-phenyl-1,2,4,5-tetrahydropyridine (MPTP) in Parkinson's disease (PD) model mice (Zhu et al., 2019). These studies indicate that apelin-13 is involved in regulating microglia polarization and neuronal autophagy, exerting neuroprotective effects. However, the specific mechanism needs to be further elucidated. We tested the hypothesis that apelin-13 ameliorated inflammatory response through modulating microglia polarization by altering autophagy. Besides, apelin-13 regulated inflammatory response by inhibiting H3K9ac enrichment at inflammatory gene promoter in LPS-stimulated microglia. Our results provide mechanistic insights into the role of apelin-13 as an underlying target for microglia inflammation suppression.

METHODS

Cell culture and treatment

BV-2 cells, received from the American Type Culture Collection (ATCC, Manassas, USA), were incubated in DMEM medium containing 10% FBS and 1% penicillin-streptomycin (Gibco, Grand Island, USA) under 5% CO_2 at 37°C, until 90% confluence. They were then separated into control, LPS, apelin-13, LPS+apelin-13, LPS+apelin-13+chloroquine (CQ) and LPS+apelin-13+valproate (VPA) groups. The BV-2 culture medium of LPS group was added with LPS (2 μg/mL) and incubated for 6 h. After addition with apelin-13 (1 μM) into the medium, apelin-13 group was cultured for 24 h. The LPS+apelin-13 group was preincubated with apelin-13 for 24 h and then cultured with LPS for 6 h. In LPS+apelin-13+CQ group, 50 μM chloroquine (CQ) was utilized for pretreating the Bv-2 cells for 2 h, followed by incubation with apelin-13 for 24 h and LPS for 6 h. Prior to treatment with apelin-13 for 24 h and LPS for 6 h, BV-2 cells of LPS+apelin-13+VPA group was treated by 1 mM histone deacetylase (HDAC) antagonist valproate (VPA) for 1 h. LPS, CQ, VPA were purchased from Sigma-Aldrich (St. Louis, MO, USA), and apelin-13 was obtained from Phoenix Pharmaceutical (Belmont, CA, USA).

Immunofluorescence

BV-2 cells, cultured on 12 mm coverslips in medium, then fixed in paraformaldehyde (4%) for 30 min. Then they were treated for 20 min with 0.1 M glycine in PBS. After permeabilization with 0.1% Triton X-100 for 5 min, the primary antibody F-actin (1:500, Abcam, Cambridge, USA) was used to incubate the cells overnight at 4°C. After washed by PBS, cells were subsequently incubated with secondary antibody (1:500, Abcam) for 1 h at room temperature followed by washed

with PBS. Finally, to highlight the nucleus, the cells were marked with DAPI. Axio Observer inverted microscope (Carl Zeiss Inc., Ober Kochen, Germany) was applied for immunofluorescence signal assessment. ImageJ software was utilized for cell areas measurement and values were presented in μm^2.

Flow cytometry

The membrane proteins of CD16/32 (M1 marker) and CD206 (M2 maker) in BV-2 cells were measured by flow cytometry. Briefly, cells were cultured in 6-well plates with a density of 1×10^6 per well and incubated with LPS, apelin-13 or CQ, alone or in combination. Then cells were collected and digested with trypsin (Beijing Solarbio Science & Technology Co., Ltd., Beijing, China), followed by centrifuging at 1000 rpm for 10 min. After washed with PBS for twice and cell pellet collection at a density of 3×10^6 cells/mL, APC anti-mouse CD16/32 (BioLegend, San Diego, USA) or APC anti-human CD206 (BioLegend) was added at 4°C and cells were treated for 0.5 h in the dark. In the end, they were washed twice with PBS, followed by re-suspended in 500 µL PBS solution. Each sample (10^5 cells) were then measured with flow cytometer (BD Biosciences, Franklin Lakes, USA) for detecting light scatter characteristics.

Quantitative reverse transcription polymerase chain reaction (qRT-PCR)

Total RNA extracted from BV-2 cells with TRIzol Reagent (Takara, Tokyo, Japan). cDNA was generated with TaqMan miRNA Reverse Transcription Kit (ThermoFisher, Waltham, USA). qRT-PCR was operated for each sample in triplicate on ABI 7500 Fast Real-Time PCR system (Applied Biosystems, Carlsbad, USA) with SYBR Green PCR Kit (Thermo Fisher Scientific). The primers were designed for real-time PCR amplification on Table 1. The data were standardized to the endogenous reference of GAPDH. The mRNA expressions of iNOS, Arg-1, IL-10, IL-6 and TNF-α were calculated with the $2^{-\Delta\Delta Ct}$ method.

Western blot

Cells were lysed with cell lysis buffer (Beyotime, Zhejiang, China) containing protease inhibitors and stored in a -80°C refrigerator. Proteins were separated with 10% SDS-PAGE followed by transferred onto PVDF membranes. After blocked with 5% non-fat milk powder in Tris-buffered saline for 1 h, they were treated, at 4°C, with primary antibody overnight. Then membranes were washed, followed by incubation at room temperature with secondary antibody for 2 h. In the end, protein bands were detected with enhanced chemiluminescence (ECL) reagents (Pierce, Rockford, IL, USA). The antibodies were as follows: anti-Beclin-1 (1:500, Bioss, Beijing, China), anti-p62 (1:500, Bioss), anti-ATG3 (1:500, Bioss), anti-ATG5 (1:500, Bioss), anti-LC3-II (1:500, Sigma Aldrich, St. Louis, USA), anti-LC3-I (1:500, Sigma Aldrich), anti-CD16/32 (1:500, BD Bioscience), anti-CD206 (1:500, BD Bioscience) and anti-GAPDH (1:1000, Sigma Aldrich).

Chromatin immunoprecipitation (ChIP)

EZ-ChIP Chromatin Immunoprecipitation Kit (Millipore, Billerica, MA, USA) was utilized for ChIP assay following the instruction. Protein-DNA was cross-linked in BV-2 cells with paraformaldehyde (1%) for 10 min followed by quenched with glycine (2.5 mM). Cells were lysed on ice, and the cross-linked DNA in crude extracts were sheared into smaller fragments (200-1000 bp) and measured with gel electrophoresis. To preclear nonspecific interactions, sheared DNA was

Table 1. Sequences of primers used in qRT-PCR.

Gene	Forward primer (5′-3′)	Reversed primer (5′-3′)
iNOS	GGGCTGTCACGGAGATCAATG	GCCCGGTACTCATTCTGCATG
Arg-1	AGGAAAGCTGGTCTGCTGGAA	AGATGCTTCCAACTGCCAGAC
IL-10	TTACCTGGTAGAAGTGATGCCC	GACACCTTGGTCTTGGAGCTTA
IL-6	CGGAGAGGAGACTTCACAGAGGA	TTTCCACGATTTCCCAGAGAACA
TNF-α	CTGAACTTCGGGGTGATCGG	GGCTTGTCACTCGAATTTTGAGA
GAPDH	GTCTTCCTTGAGCACCTGGATC	GTCTTCCTTGAGCACCTGGATC

incubated with protein agarose/salmon sperm (Beyotime) beads. After that, they were incubated, at 4°C, with IgG (Gibco) and antibody H3K9ac (Gibco) under shaking overnight. Then crosslinking was reversed and the QIAquick PCR purification Kit (Qiagen, Hilden, Germany) was utilized to purify the immunoprecipitated DNA fragments.

Statistical analysis

The experimental results were exhibited with mean ± SD from at least three independent experiments. The statistical analysis was analyzed on GraphPad Prism 8 software. Comparison between groups was performed by Student's t-test. Comparison among three or more groups was conducted using one-way ANOVA followed by Tukey's *post hoc* test. Statistically significant difference was presented with *P<0.05.

RESULTS

Apelin-13 alleviates microglia activation induced by LPS

To investigate apelin-13 impact on LPS-treated BV-2 cells, immunofluorescence analysis with F-actin staining was applied. In control group, cells presented classic morphology, being unipolar with one or more processes. After LPS treatment, the surface area of BV-2 cells was obviously increased and more flat forms of actin markers were observed (P<0.05). And in apelin-13+LPS group, the surface area of BV-2 cells was decreased apparently and LPS-stimulated ameboid phenotype was reversed, in comparison to LPS group (P<0.05) [$F_{3,8}$=17.52, P=0.0007]. There was no significance between apelin-13 and apelin-13+LPS groups (Fig. 1A, B). These findings suggested apelin-13 alleviated microglia activation induced by LPS.

Apelin-13 alleviates inflammatory response through regulating LPS-induced microglia polarization and autophagy

To explore whether apelin-13 could regulate the LPS-induced microglia polarization and autophagy to reduce inflammatory response, BV-2 cells, stimulated with or without LPS, were treated with or without apelin-13. The western blot results presented that expression of p62 ($F_{3,8}$=18.65, P=0.0006) was increased and expressions of Beclin-1 ($F_{3,8}$=27.36, P=0.0001), ATG3 ($F_{3,8}$=11.78, P=0.0026) and ATG5 ($F_{3,8}$=13.47, P=0.0017) were decreased in LPS group. Besides, the ratio of LC3-II/LC3-I ($F_{3,8}$=73.50, P<0.0001) was also decreased in LPS group. These alterations were reversed by apelin-13 treatment (Fig. 2A). To evaluate microglia polarization, CD16/32 and CD206 was employed as M1 and M2 polarization markers, respectively (Zhang et al.,

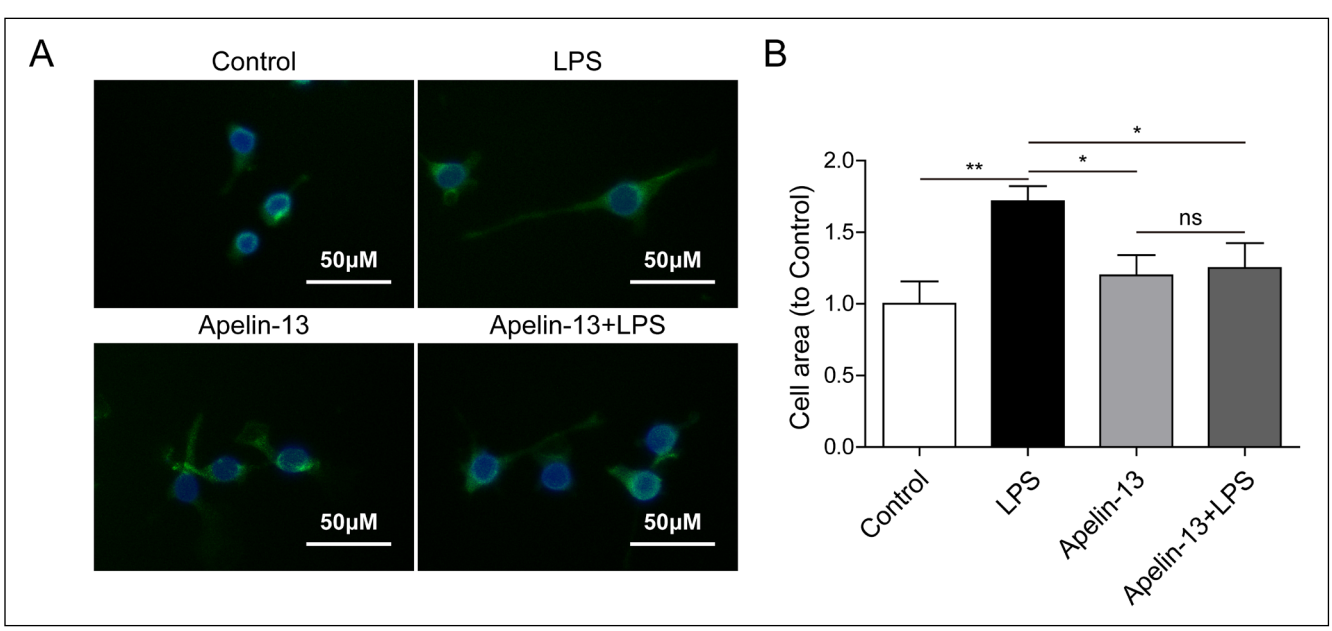

Fig. 1. Apelin-13 alleviates microglia activation induced by LPS in BV-2 cells. (A) The BV-2 cell morphology was analyzed with F-actin to highlight actin. (B) The BV-2 cell area was analyzed with ImageJ software. Scale bar=50 μm. Results were presented as mean ± SD. n=3, one-way ANOVA followed by Tukey's *post hoc* test, **P<0.01, n.s means P>0.05.

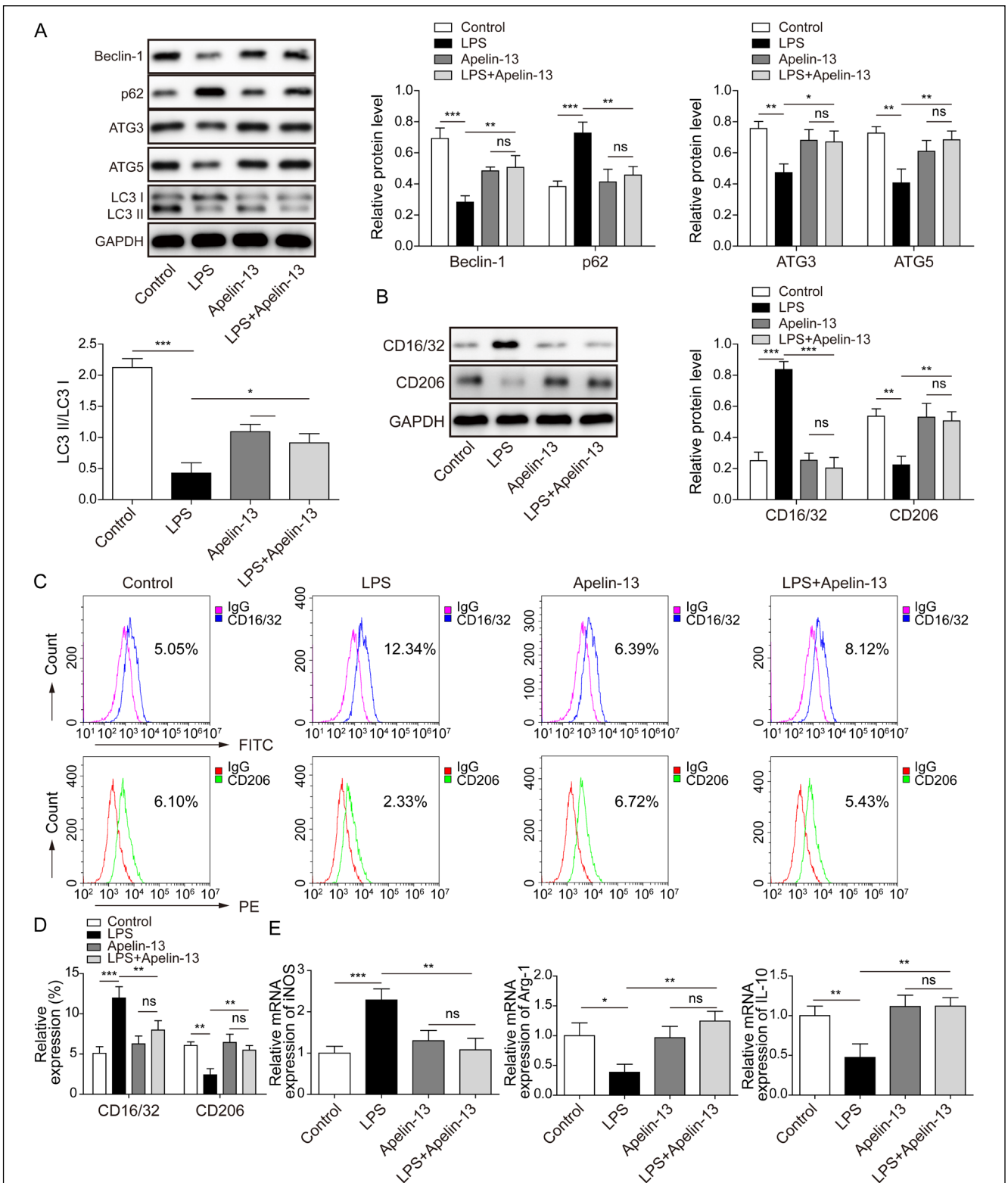

Fig. 2. Apelin-13 alleviates inflammatory response through regulating LPS-induced microglia polarization and autophagy in BV-2 cells. (A) Expression of Beclin-1, P62, ATG3, ATG5, LC3-II and LC3-I were detected by western blot. M1 marker CD16/32 expression and M2 marker CD206 expression were measured with western blot (B) and flow cytometry (C, D). Level of pro-inflammatory cytokine iNOS as well as anti-inflammatory cytokines Arg-1 and IL-10 were analyzed with qRT-PCR (E). Results were presented as mean ± SD. n=3, one-way ANOVA followed by Tukey's *post hoc* test, **P*<0.05, ***P*<0.01, ****P*<0.001, n.s means *P*>0.05.

2019). Expression of CD16/32 (M1 marker) and CD206 (M2 maker) in BV-2 cells were examined by western blot (Fig. 2B) [CD16/32, $F_{3,8}$=87.92, P<0.0001; CD206, $F_{3,8}$=16.51, P=0.0009] and flow cytometry (Fig. 2C, D) [CD16/32, $F_{3,8}$=21.80, P=0.0003; CD206, $F_{3,8}$=18.54, P=0.0006] to determine the effect of apelin-13 on microglia polarization in LPS-treated BV2 cells. The results presented the increased CD16/32 expression and decreased CD206 expression induced by LPS, while apelin-13 treatment down-regulated CD16/32 expression and up-regulated CD206 expression in LPS-induced BV-2 cells (P<0.05). In inflammatory response examination, LPS promoted the expression of pro-inflammatory cytokine iNOS and inhibited the expression of anti-inflammatory cytokines Arg-1 and IL-10, while apelin-13 treatment restored the variation of iNOS, Arg-1 and IL-10 detected by qRT-PCR (Fig. 2E) [iNOS, $F_{3,8}$=17.60, P=0.0007; Arg-1, $F_{3,8}$=12.51, P=0.0022; IL-10, $F_{3,8}$=15.02, P=0.0012]. No significance was observed between apelin-13 and apelin-13+LPS groups (Fig. 2A-E). These findings suggested apelin-13 played an inhibitory role on inflammatory response *via* regulating microglia polarization and autophagy induced by LPS.

Blocking apelin-13-induced autophagy promotion can enhance M1 polarization and reduce M2 polarization, thereby promoting inflammatory response

We suppressed autophagy with CQ and then explored the effect of apelin-13 on autophagy, microglia polarization and inflammatory response. The expression of p62 was elevated, while the expression of Beclin-1, ATG3 and ATG5 was reduced after CQ administration with western blot assay, compared with LPS+apelin-13 group (P<0.05). The ratio of LC3-II/LC3-I was also down-regulated with CQ supply, in comparison with LPS+apelin-13 group (P<0.05). The results demonstrated that the promotive effect of apelin-13 on autophagy was reduced by CQ administrated (Fig. 3A) [Beclin-1, $F_{3,8}$=14.72, P=0.0013; p62, $F_{3,8}$=16.68, P=0.0008; ATG3, $F_{3,8}$=15.71, P=0.0010; ATG5, $F_{3,8}$=20.32, P=0.0004]. Apelin-13 significantly down-regulated the M1 marker CD16/32 level and obviously up-regulated M2 marker CD206 level, however these effects were effectively reversed with CQ treatment evaluated by western blot (Fig. 3B) [CD16/32, $F_{3,8}$=18.56, P=0.0006; CD206, $F_{3,8}$=47.47, P<0.0001] and flow cytometry (Fig. 3C, D) [CD16/32, $F_{3,8}$=31.11, P<0.0001; CD206, $F_{3,8}$=20.91, P=0.0004]. Furthermore, compared to the apelin-13 administration, co-treatment with CQ and apelin-13 led to increased iNOS and decreased Arg-1 and IL-10 by qRT-PCR (Fig. 3E) [iNOS, $F_{3,8}$=35.82, P<0.0001; Arg-1, $F_{3,8}$=22.58, P=0.0003; IL-10, $F_{3,8}$=13.84, P=0.0016]. Collectively, these results suggested that the autophagy inhibitor CQ could block apelin-13-induced autophagy promotion, which enhanced M1 polarization and reduced M2 polarization, promoting inflammatory response.

Apelin-13 decreases the enrichment of H3K9ac at the promoter region of TNF-α and IL-6 inhibiting inflammatory response

The variation of H3K9ac enrichment at promoters of genes TNF-α and IL-6 was explored in BV-2 cells. The ChIP analysis demonstrated H3K9ac/H3 levels at TNF-α and IL-6 gene promoter were evidently increased in LPS-induced BV-2 microglia, and apelin-13 treatment effectively decreased (Fig. 4A) [TNF-α, $F_{3,8}$=15.63, P=0.0010; IL-6, $F_{3,8}$=12.75, P=0.0020]. Consistently, our results showed an apparent up-regulation of TNF-α and IL-6 mRNA expression in LPS-induced microglia compared with the control group with qRT-PCR detection. Additionally, apelin-13 treatment resulted in the decreased mRNA expression of TNF-α and IL-6 (P<0.05) (Fig. 4B) [TNF-α, $F_{3,8}$=21.90, P=0.0003; IL-6, $F_{3,8}$=32.46, P<0.0001]. The levels of H3K9ac/H3 at TNF-α and IL-6 gene promoter have no significance between apelin-13 and apelin-13+LPS groups, as well as TNF-α and IL-6 mRNA expressions (Fig. 4 A, B). These results indicated that apelin-13 modulated the inflammatory response through regulating enrichment of H3K9ac on TNF-α and IL-6 promoter region.

VPA inhibits the effect of apelin-13 on enrichment of H3K9ac at the promoter region of TNF-α and IL-6

To further explore the impact of histone deacetylase (HDAC) antagonist sodium valproate (VPA) on apelin-13 inhibitory effect of H3K9ac enrichment at promoter region of TNF-α and IL-6, ChIP analysis was utilized. The results of ChIP assay exhibited that apelin-13 declined the H3K9ac enrichment in BV-2 cells induced by LPS, while these impacts were diminished after VPA treatment (Fig. 5A) [TNF-α, $F_{3,8}$=18.36, P=0.0006; IL-6, $F_{3,8}$=25.13, P=0.0002]. Identically, findings presented an obvious up-regulation of TNF-α and IL-6 after co-treatment of VPA and apelin-13, compared with apelin-13 treatment in LPS-induced BV-2 cells (Fig. 5B) [TNF-α, $F_{3,8}$=28.31, P=0.0001; IL-6, $F_{3,8}$=29.74, P=0.0001]. It indicated that VPA inhibited the impact of apelin-13 on H3K9ac enrichment of TNF-α and IL-6 promoter region and expression of TNF-α and IL-6.

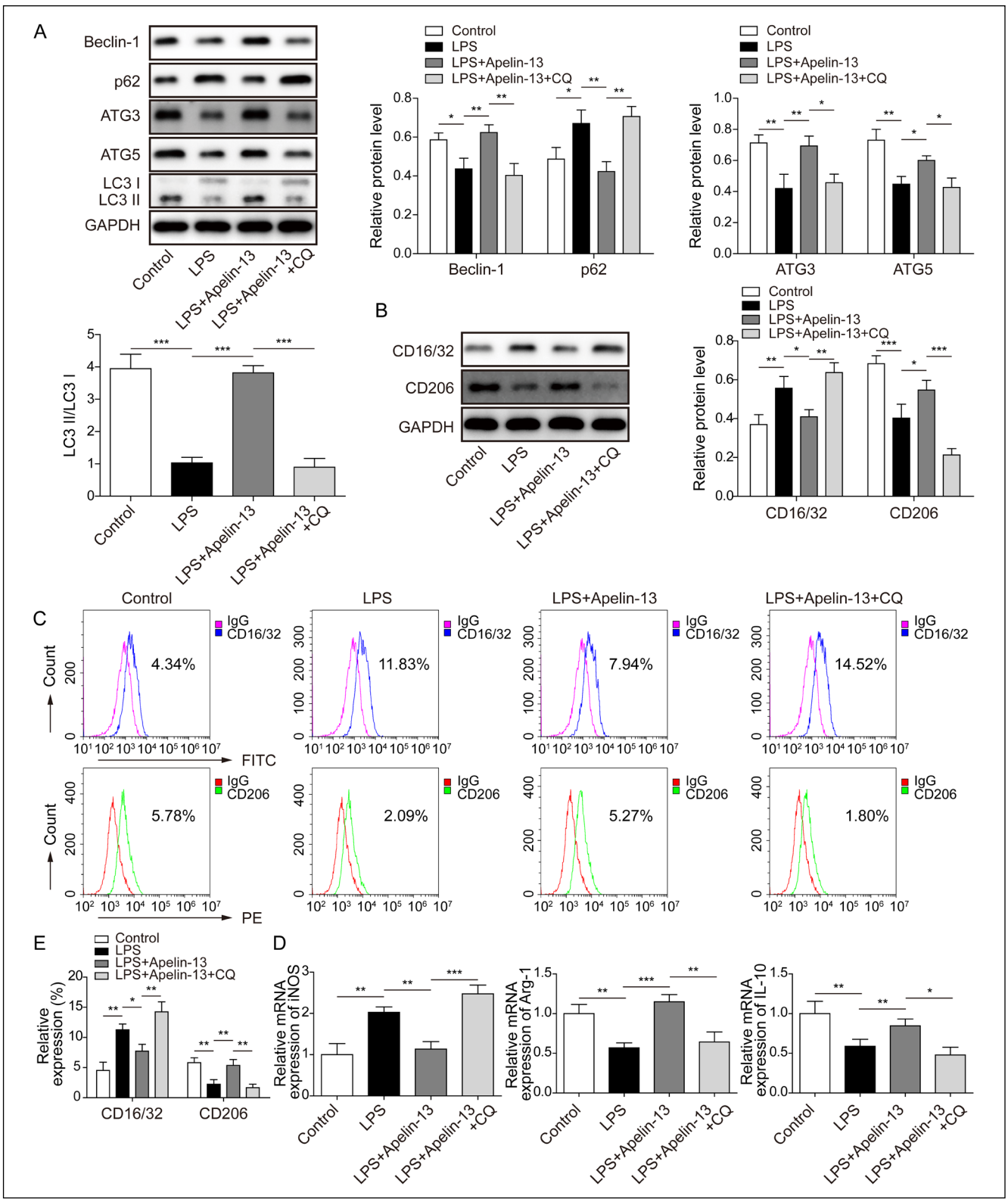

Fig. 3. Blocking Apelin-13-induced autophagy promotion can enhance M1 polarization and reduce M2 polarization, thereby promoting inflammatory response in BV-2 cells treated by LPS. (A) Level of Beclin-1, P62, ATG3, ATG5, LC3-II and LC3-I, as well as (B) CD16/32 (M1 marker) level and CD206 (M2 maker) level were valued by western blot. (C, D) Flow cytometry was utilized to detect the level of CD16/32 (M1 marker) and CD206 (M2 maker). (E) qRT-PCR was applied for analyzing expression of iNOS as well as levels of Arg-1 and IL-10. Results were presented as mean ± SD. n=3, one-way ANOVA followed by Tukey's *post hoc* test, **P*<0.05, ***P*<0.01, ****P*<0.001.

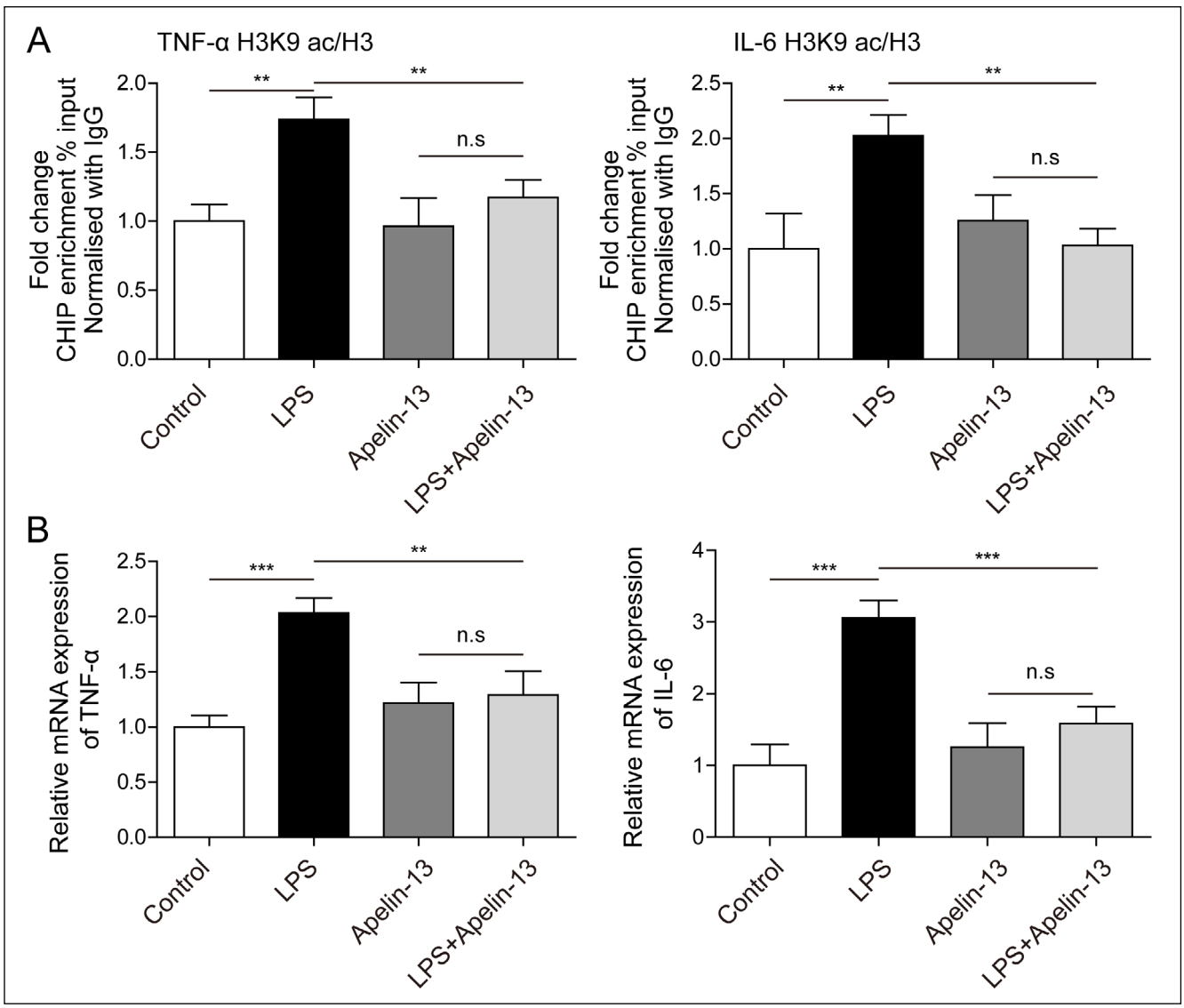

Fig. 4. Apelin-13 decreases the enrichment of H3K9ac at the promoter region of TNF-α and IL-6 and inhibits inflammatory response in LPS-treated BV-2 cells. (A) H3K9ac/H3 enrichment was observed at gene promoters of TNF-α and IL-6 with ChIP assay. (B) qRT-PCR was applied to measure the mRNA expression of TNF-α and IL-6. Results were presented as mean ± SD. n=3, one-way ANOVA followed by Tukey's *post hoc* test, ***P*<0.01, ****P*<0.001, n.s means *P*>0.05.

DISCUSSION

In central nervous system (CNS), microglia are generally kept in a quiescent state. Studies of microglia have defined specific activation states: M1 (classical activation) and M2 (alternative activation), and they perform diverse functions, either beneficial or harmful, after activated (Boche et al., 2013). For instance, during the development of multiple sclerosis, microglia are expressed as M1 phenotype in early stage, releasing proinflammatory cytokines, leading to tissue damage, while in later stage, most microglia become M2 phenotype, related with inflammation reduction and tissue repair (Chu et al., 2018). Exist studies demonstrate that M1/M2 phenotype balance plays a significant role in disease progression. We found that in LPS-stimulated microglia, apelin-13 administration could alter the expression of autophagy associated proteins, regulating M1 and M2 phenotype of microglia, leading to pro-inflammatory cytokines suppression. Additionally, H3K9ac enrichment at TNF-α and IL-6 promoter was reduced following apelin-13 treatment. We hereby demonstrate that *via* suppression of H3K9ac enrichment or shifting microglia from M1 to M2 phenotype by facilitating autophagy, apelin-13 ameliorates microglia inflammation following LPS stimulation.

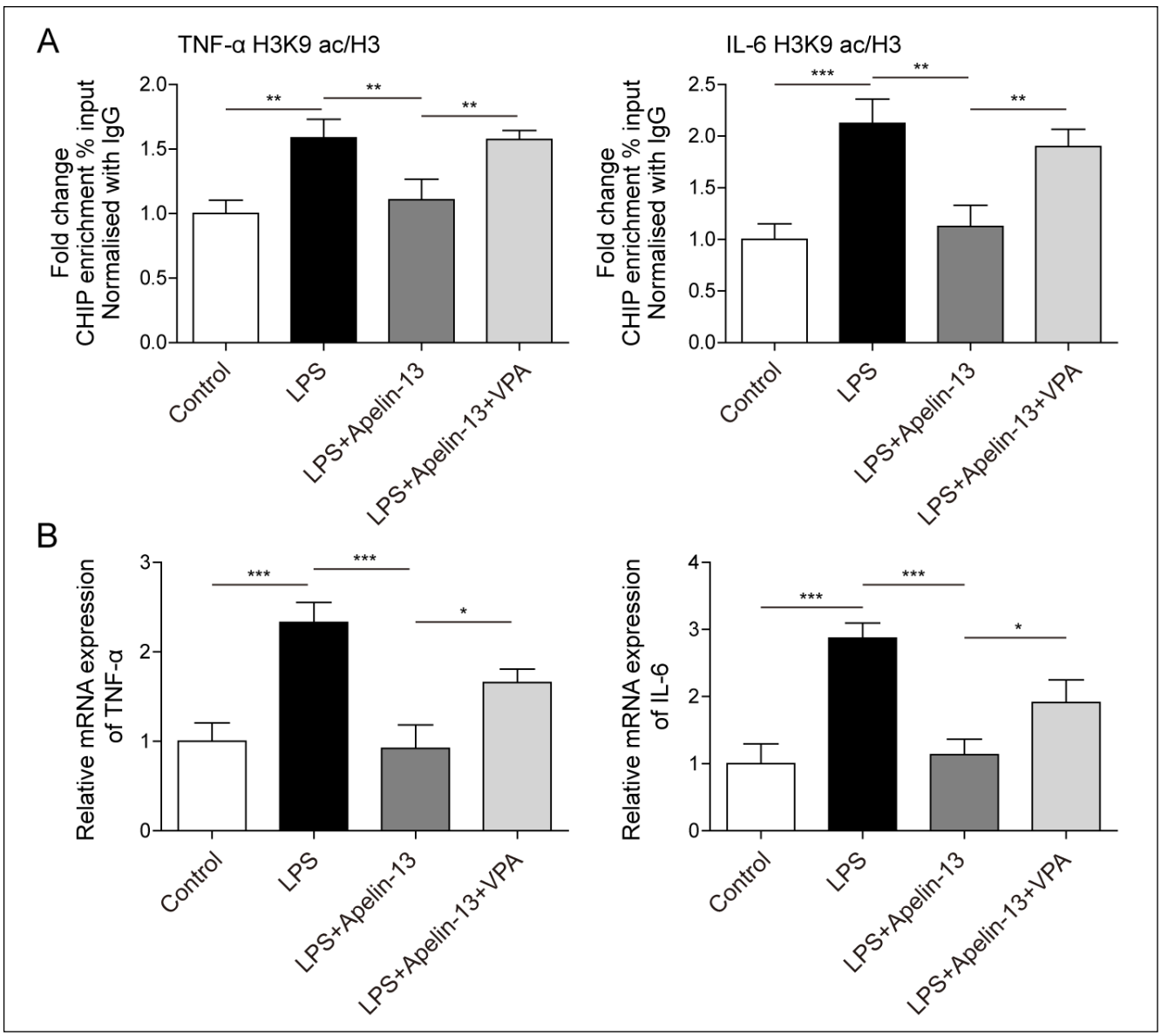

Fig. 5. VPA inhibits the effect of Apelin-13 on enrichment of H3K9ac at the promoter region of TNF-α and IL-6 in BV-2 cells incubated with LPS. (A) ChIP assay was applied to evaluate the enrichment of H3K9ac at TNF-α and IL-6 promoter region. (B) The TNF-α and IL-6 mRNA expressions were measured by qRT-PCR. Results were presented as mean ± SD. n=3, one-way ANOVA followed by Tukey's *post hoc* test, **P*<0.05, ***P*<0.01, ****P*<0.001.

Microglia activation, part of CNS innate immune defense, is involved in neuroinflammatory responses (Glezer et al., 2007; Kumar et al., 2013). Previous study has proved that M1 microglia may lead to the neurotrophic system dysfunction by expressing pro-inflammatory cytokines such as IL-1β, IL-6 and TNF-α (Wang et al., 2015). Furthermore, M2 phenotype plays a neuroprotective role and ameliorates inflammation-induced damage in CNS (Pisanu et al., 2014). Inhibition of M1 microglia polarization contributes to decreasing necroptosis of oligodendrocytes after SCI (Fan et al., 2019). However, shifting from M1 to M2 phenotype alleviates neuronal degeneration and demyelination, while promotes oligodendrocyte precursor cell maturation (Han et al., 2018). Apelin-13, a small bioactive peptide, exerts neuroprotective effects through promoting anti-inflammation (Cheng et al., 2012; Xin et al., 2015). Microglia, including BV-2 microglia cell line, can be stimulated by LPS to M1 phenotype for expressing pro-inflammatory cytokines (Orihuela et al., 2016). It remains elusive that whether apelin-13 can transform microglia polarization against LPS-induced inflammatory *via* modulating autophagy in microglia. Therefore, we first investigated microglia polarization in BV2 cells

of LPS-induced inflammatory response after LPS stimulation or combined with apelin-13 treatment. We found that after apelin-13 supply, CD16/32 level was decreased and CD206 level was increased, indicating the microglia polarization toward M2 status in cultured BV-2 cells. Apelin-13 supply significantly increased level of Arg-1 (M2-type marker) and elevated secretion of anti-inflammatory factors, such as IL-4 and IL-10, resulting in ameliorating depression-like behavior in chronic stress rats (Zhou et al., 2020). Research has verified that, apelin-13 exerts anti-neuroinflammatory effects in N9 microglia by shifting microglia to M2 phenotype through STAT3 signaling pathway (Zhou et al., 2019). Our study, together with these previous studies, confirmed that apelin-13 could promote M2 phenotype switch in activated microglia.

Study has demonstrated that autophagy is participated in various physiological and pathological cellular processes. For example, it is indicated that autophagy is involved in cell differentiation of vascular smooth muscle cells (VSMCs) (Peng et al., 2017). Besides, PKCδ inhibition protects kidney tubular cells by upregulating autophagy (Zhang et al., 2017). In central nervous system, the enhanced autophagy by rapamycin and resveratrol can facilitate microglia activating towards M2 status and alleviate TNF-α-induced microglia neurotoxicity (Jin et al., 2018). Antagonizing peroxisome proliferator-activated receptor γ (PPAR-γ) improves autophagy, promoting M1-to-M2 shift of microglia (Ji et al., 2018). Apelin-13 is proved to protect dopaminergic neurons at least partially by promoting autophagy in MPTP-treated mice of Parkinson's disease model (Zhu et al., 2019). Besides, apelin-13 can activate autophagy to restore autophagy impairment induced by rotenone in SH-SY5Y cells (Chen et al., 2020). Apelin-13 induced autophagy, elevated the protein expressions of LC3-II/I and Beclin-1 in human umbilical vein endothelial cells (HUVECs) (Liu et al., 2018). Alteration of autophagy can either induce or inhibit inflammatory response in microglia (Su et al., 2016). Suppression of autophagic flux modulates microglia to M1 phenotype with increased cyclooxygenase-2 (COX-2), iNOS and TNF-α in BV-2 cells (Xia et al., 2016). We discovered that apelin-13 enhanced autophagy in LPS treated cells by detecting the autophagy associated proteins expression. In addition, we found that autophagy inhibitor CQ promoted M1 polarization of microglia, blocking the anti-inflammation effects of apelin-13. Our findings illustrated a mechanism of apelin-13 in alleviating inflammatory response *via* microglia polarization to M2 status induced by autophagy enhancement.

HDAC inhibitors block the changes of glioma-conditioned medium-induced histone modifications, restoring microglia ability of initiating inflammatory responses (Maleszewska et al., 2020). The classical HDAC inhibitor valproic acid (VPA) is a broad spectrum antiepileptic drug, which nonspecifically inhibits classes I and II a HDAC proteins (Russo et al., 2020). H3K9ac, a histone modification modulated by HDACs, is enriched at inducible and active gene promoters (Peterson and Laniel, 2004). Previous research reveals that sodium butyrate, HDAC class I and II inhibitor, alters H3K9ac enrichment and transcription at the promoters of anti-inflammatory (IL-10) and pro-inflammatory (TNF-α and IL-6) genes in microglia (Patnala et al., 2017). Enrichment of H3K9ac on promoters of IL-6 and TNF-α after alcohol exposure at early life in rats, acts as a marker for cellular memory of microglia in immune event, leading to hyper-inflammatory response for immune challenges in later life (Chastain et al., 2019). We found that apelin-13 inhibits H3K9ac enrichment in the inflammatory gene promoter region of TNF-α and IL-6 and the expression of TNF-α and IL-6 was apparently declined. This effect could be blocked by VPA, HDAC antagonist. Apelin-13 is reported to up-regulate BDNF/TrkB pathway in sporadic Alzheimer's disease against cognitive impairments through reducing expression of inflammatory factors (IL-1β and TNF-α) (Luo et al., 2019). Apelin-13 exerts protective function on neurons through reducing levels of inflammatory cytokines such as TNF-α and IL-1β (Xin et al., 2015). Similar with the above studies, our research revealed a mechanism of apelin-13 on reducing inflammatory response *via* down-regulation of H3K9ac enrichment in promoter region of TNF-α and IL-6 in LPS stimulated microglia. We hence reason that in microglia stimulated by LPS, Apelin-13 impact on inflammatory reaction is depended on epigenetic mechanism.

CONCLUSION

In conclusion, our research proves that apelin-13 exerts the inhibitory effects on inflammatory response of microglia *via* promoting switch from M1 to M2 phenotype due to autophagy enhancement and suppressing H3K9ac enrichment at TNF-α and IL-6 promoter regions. The present study represents an encouraging strategy of apelin-13 for neurological injury *via* modulating inflammatory response of microglia.

ACKNOWLEDGEMENTS

This work was supported by Natural Science Foundation of Hunan province-surface project (No.2021JJ31036), Natural Science Foundation-Kewei

joint project of Hunan Province (No.2021JJ70070), Hunan Provincial Health Commission Scientific Research Project (No.202205014861).

REFERENCES

An J, Chen B, Kang X, Zhang R, Guo Y, Zhao J, Yang H (2020) Neuroprotective effects of natural compounds on LPS-induced inflammatory responses in microglia. Am J Transl Res 12: 2353–2378.

Boche D, Perry VH, Nicoll JA (2013) Review: activation patterns of microglia and their identification in the human brain. Neuropathol Appl Neurobiol 39: 3–18.

Chastain LG, Franklin T, Gangisetty O, Cabrera MA, Mukherjee S, Shrivastava P, Jabbar S, Sarkar DK (2019) Early life alcohol exposure primes hypothalamic microglia to later-life hypersensitivity to immune stress: possible epigenetic mechanism. Neuropsychopharmacology 44: 1579–1588.

Chen P, Wang Y, Chen L, Song N, Xie J (2020) Apelin-13 protects dopaminergic neurons against rotenone-induced neurotoxicity through the AMPK/mTOR/ULK-1 mediated autophagy activation. Int J Mol Sci 21: 8376.

Cheng B, Chen J, Bai B, Xin Q (2012) Neuroprotection of apelin and its signaling pathway. Peptides 37: 171–173.

Chu F, Shi M, Zheng C, Shen D, Zhu J, Zheng X, Cui L (2018) The roles of macrophages and microglia in multiple sclerosis and experimental autoimmune encephalomyelitis. J Neuroimmunol 318: 1–7.

Do HTT, Bui BP, Sim S, Jung JK, Lee H, Cho J (2020) Anti-Inflammatory and anti-migratory activities of isoquinoline-1-carboxamide derivatives in LPS-treated BV2 microglial cells via inhibition of MAPKs/NF-kB pathway. Int J Mol Sci 21: 2319.

Fan H, Tang HB, Shan LQ, Liu SC, Huang DG, Chen X, Chen Z, Yang M, Yin XH, Yang H, Hao DJ (2019) Quercetin prevents necroptosis of oligodendrocytes by inhibiting macrophages/microglia polarization to M1 phenotype after spinal cord injury in rats. J Neuroinflammation 16: 206.

Glezer I, Simard AR, Rivest S (2007) Neuroprotective role of the innate immune system by microglia. Neuroscience 147: 867–883.

Han D, Yu Z, Liu W, Yin D, Pu Y, Feng J, Yuan Y, Huang A, Cao L, He C (2018) Plasma Hemopexin ameliorates murine spinal cord injury by switching microglia from the M1 state to the M2 state. Cell Death Dis 9: 181.

Hu X, Li P, Guo Y, Wang H, Leak RK, Chen S, Gao Y, Chen J (2012) Microglia/macrophage polarization dynamics reveal novel mechanism of injury expansion after focal cerebral ischemia. Stroke 43: 3063–3070.

Ji J, Xue TF, Guo XD, Yang J, Guo RB, Wang J, Huang JY, Zhao XJ, Sun XL (2018) Antagonizing peroxisome proliferator-activated receptor gamma facilitates M1-to-M2 shift of microglia by enhancing autophagy via the LKB1-AMPK signaling pathway. Aging Cell 17: e12774.

Jin MM, Wang F, Qi D, Liu WW, Gu C, Mao CJ, Yang YP, Zhao Z, Hu LF, Liu CF (2018) A critical role of autophagy in regulating microglia polarization in neurodegeneration. Front Aging Neurosci 10: 378.

Kobashi S, Terashima T, Katagi M, Nakae Y, Okano J, Suzuki Y, Urushitani M, Kojima H (2020) Transplantation of M2-deviated microglia promotes recovery of motor function after spinal cord injury in mice. Mol Ther 28: 254–265.

Kumar A, Stoica BA, Sabirzhanov B, Burns MP, Faden AI, Loane DJ (2013) Traumatic brain injury in aged animals increases lesion size and chronically alters microglial/macrophage classical and alternative activation states. Neurobiol Aging 34: 1397–1411.

Liu M, Li H, Zhou Q, Zhao H, Lv D, Cao J, Jiang J, Tang M, Wu D, Liu J, Wu L, Hu H, He L, Huang S, Chen Z, Li L, Chen L (2018) ROS-autophagy pathway mediates monocytes-human umbilical vein endothelial cells adhesion induced by apelin-13. J Cell Physiol 233: 6839–6850.

Livingston MJ, Dong Z (2014) Autophagy in acute kidney injury. Semin Nephrol 34: 17–26.

Luo H, Xiang Y, Qu X, Liu H, Liu C, Li G, Han L, Qin X (2019) Apelin-13 suppresses neuroinflammation against cognitive deficit in a streptozotocin-induced rat model of Alzheimer's disease through activation of BDNF-TrkB signaling pathway. Front Pharmacol 10: 395.

Ma K, Guo J, Wang G, Ni Q, Liu X (2020) Toll-like receptor 2-mediated autophagy promotes microglial cell death by modulating the microglial M1/M2 phenotype. Inflammation 43: 701–711.

Maleszewska M, Steranka A, Smiech M, Kaza B, Pilanc P, Dabrowski M, Kaminska B (2020) Sequential changes in histone modifications shape transcriptional responses underlying microglia polarization by glioma. Glia 69: 109–123.

Nam HY, Nam JH, Yoon G, Lee JY, Nam Y, Kang HJ, Cho HJ, Kim J, Hoe HS (2018) Ibrutinib suppresses LPS-induced neuroinflammatory responses in BV2 microglial cells and wild-type mice. J Neuroinflammation 15: 271.

Orihuela R, McPherson CA, Harry GJ (2016) Microglial M1/M2 polarization and metabolic states. Br J Pharmacol 173: 649–665.

Patnala R, Arumugam TV, Gupta N, Dheen ST (2017) HDAC inhibitor sodium butyrate-mediated epigenetic regulation enhances neuroprotective function of microglia during ischemic stroke. Mol Neurobiol 54: 6391–6411.

Peng YQ, Xiong D, Lin X, Cui RR, Xu F, Zhong JY, Zhu T, Wu F, Mao MZ, Liao XB, Yuan LQ (2017) Oestrogen inhibits arterial calcification by promoting autophagy. Sci Rep 7: 3549.

Peterson CL, Laniel MA (2004) Histones and histone modifications. Curr Biol 14: R546–551.

Pisanu A, Lecca D, Mulas G, Wardas J, Simbula G, Spiga S, Carta AR (2014) Dynamic changes in pro- and anti-inflammatory cytokines in microglia after PPAR-gamma agonist neuroprotective treatment in the MPTPp mouse model of progressive Parkinson's disease. Neurobiol Dis 71: 280–291.

Russo R, Kemp M, Bhatti UF, Pai M, Wakam G, Biesterveld B, Alam HB (2020) Life on the battlefield: Valproic acid for combat applications. J Trauma Acute Care Surg 89: S69-S76.

Song Y, Li Z, He T, Qu M, Jiang L, Li W, Shi X, Pan J, Zhang L, Wang Y, Zhang Z, Tang Y, Yang GY (2019) M2 microglia-derived exosomes protect the mouse brain from ischemia-reperfusion injury via exosomal miR-124. Theranostics 9: 2910–2923.

Su P, Zhang J, Wang D, Zhao F, Cao Z, Aschner M, Luo W (2016) The role of autophagy in modulation of neuroinflammation in microglia. Neuroscience 319: 155–167.

Tang Y, Le W (2016) Differential roles of M1 and M2 microglia in neurodegenerative diseases. Mol Neurobiol 53: 1181–1194.

Wang C, Wang Q, Lou Y, Xu J, Feng Z, Chen Y, Tang Q, Zheng G, Zhang Z, Wu Y, Tian N, Zhou Y, Xu H, Zhang X (2018) Salidroside attenuates neuroinflammation and improves functional recovery after spinal cord injury through microglia polarization regulation. J Cell Mol Med 22: 1148–1166.

Wang WY, Tan MS, Yu JT, Tan L (2015) Role of pro-inflammatory cytokines released from microglia in Alzheimer's disease. Ann Transl Med 3: 136.

Wolf SA, Boddeke HW, Kettenmann H (2017) Microglia in physiology and disease. Annu Rev Physiol 79: 619–643.

Xia CY, Zhang S, Chu SF, Wang ZZ, Song XY, Zuo W, Gao Y, Yang PF, Chen NH (2016) Autophagic flux regulates microglial phenotype according to the time of oxygen-glucose deprivation/reperfusion. Int Immunopharmacol 39: 140–148.

Xin Q, Cheng B, Pan Y, Liu H, Yang C, Chen J, Bai B (2015) Neuroprotective effects of apelin-13 on experimental ischemic stroke through suppression of inflammation. Peptides 63: 55–62.

Xu W, Li T, Gao L, Zheng J, Yan J, Zhang J, Shao A (2019) Apelin-13/APJ system attenuates early brain injury via suppression of endoplasmic reticulum stress-associated TXNIP/NLRP3 inflammasome activation and oxidative stress in a AMPK-dependent manner after subarachnoid hemorrhage in rats. J Neuroinflammation 16: 247.

Ye X, Zhu M, Che X, Wang H, Liang XJ, Wu C, Xue X, Yang J (2020) Lipopolysaccharide induces neuroinflammation in microglia by activating the MTOR pathway and downregulating Vps34 to inhibit autophagosome formation. J Neuroinflammation 17: 18.

Yu T, Yu H, Zhang B, Wang D, Li B, Zhu J, Zhu W (2019) Promising neuroprotective function for M2 microglia in kainic acid-induced neurotoxicity via the down-regulation of NF-kB and caspase 3 signaling pathways. Neuroscience 406: 86–96.

Zhang D, Pan J, Xiang X, Liu Y, Dong G, Livingston MJ, Chen JK, Yin XM, Dong Z (2017) Protein kinase cdelta suppresses autophagy to induce kidney cell apoptosis in cisplatin nephrotoxicity. J Am Soc Nephrol 28: 1131–1144.

Zhang J, Liu Q, Hu X, Fang Z, Huang F, Tang L, Zhou S (2015) Apelin/APJ signaling promotes hypoxia-induced proliferation of endothelial progenitor cells via phosphoinositide-3 kinase/Akt signaling. Mol Med Rep 12: 3829–3834.

Zhang J, Zheng Y, Luo Y, Du Y, Zhang X, Fu J (2019) Curcumin inhibits LPS-induced neuroinflammation by promoting microglial M2 polarization via TREM2/ TLR4/ NF-kappaB pathways in BV2 cells. Mol Immunol 116: 29–37.

Zhou S, Chen S, Xie W, Guo X, Zhao J (2020) Microglia polarization of hippocampus is involved in the mechanism of Apelin-13 ameliorating chronic water immersion restraint stress-induced depression-like behavior in rats. Neuropeptides 81: 102006.

Zhou S, Guo X, Chen S, Xu Z, Duan W, Zeng B (2019) Apelin-13 regulates LPS-induced N9 microglia polarization involving STAT3 signaling pathway. Neuropeptides 76: 101938.

Zhu J, Dou S, Jiang Y, Chen J, Wang C, Cheng B (2019) Apelin-13 protects dopaminergic neurons in MPTP-induced Parkinson's disease model mice through inhibiting endoplasmic reticulum stress and promoting autophagy. Brain Res 1715: 203–212.

Zhuang X, Yu Y, Jiang Y, Zhao S, Wang Y, Su L, Xie K, Yu Y, Lu Y, Lv G (2020) Molecular hydrogen attenuates sepsis-induced neuroinflammation through regulation of microglia polarization through an mTOR-autophagy-dependent pathway. Int Immunopharmacol 81: 106287.